

RESEARCH LETTER

10.1002/2016GL072457

Key Points:

- Raman analysis detects increased carbonization in pseudotachylytes
- Increased carbonization in pseudotachylytes occurs in a very short time and is preserved after alteration
- Coseismic shear stress is estimated from Raman data in pseudotachylytes

Supporting Information:

- Supporting Information S1

Correspondence to:

K. Ujiie,
kujie@geol.tsukuba.ac.jp

Citation:

Ito, K., K. Ujiie, and H. Kagi (2017), Detection of increased heating and estimation of coseismic shear stress from Raman spectra of carbonaceous material in pseudotachylytes, *Geophys. Res. Lett.*, 44, 1749–1757, doi:10.1002/2016GL072457.



Received 7 NOV 2016

Accepted 11 FEB 2017

Accepted article online 14 FEB 2017

Published online 22 FEB 2017

Detection of increased heating and estimation of coseismic shear stress from Raman spectra of carbonaceous material in pseudotachylytes

Keisuke Ito¹, Kohtaro Ujiie^{2,3} , and Hiroyuki Kagi⁴ 
¹College of Geoscience, School of Life and Environmental Sciences, University of Tsukuba, Tsukuba, Japan, ²Graduate School of Life and Environmental Sciences, University of Tsukuba, Tsukuba, Japan, ³Research and Development Center for Ocean Drilling Science, Japan Agency for Marine-Earth Science and Technology, Yokohama, Japan, ⁴Geochemical Research Center, Graduate School of Science, University of Tokyo, Tokyo, Japan

Abstract Frictional heat generated during earthquakes provides insight into the coseismic fault strength. To detect increased heating associated with faulting at seismic slip rates, we analyzed the Raman spectra of carbonaceous material in natural and experimental pseudotachylytes derived from argillite. The results indicate that the increased carbonization in pseudotachylytes relative to the host rocks could be detected when the ambient temperature is lower than 280°C. This increased carbonization can occur in ~4–16 s and is preserved even after alteration of pseudotachylytes. The comparison between experiment and Raman data demonstrated that there is a correlation between the average shear stress and the Raman spectra in pseudotachylytes. The average coseismic shear stress estimated from the correlation was 1.8 MPa. The resulting apparent friction coefficient under hydrostatic conditions at depths of 4–6 km was ~0.03–0.05. Raman analysis of carbonaceous material-bearing pseudotachylytes will be useful for estimation of coseismic fault strength.

1. Introduction

Detection of frictional heating and estimation of coseismic shear stress on faults are keys to assessing earthquake dynamics. Although seismological methods can retrieve seismic moment and stress changes, it is difficult to constrain the dynamic stress during an earthquake. Recently, borehole temperature measurements successfully estimated the coseismic shear stress from the residual heat of the 2011 Tohoku-Oki earthquake ($M_w=9.0$), which is consistent with the value determined from high-velocity friction experiments on fault zone material [Fulton *et al.*, 2013; Ujiie *et al.*, 2013]. However, there have been very few opportunities to measure fault temperatures after an earthquake. Pseudotachylytes (solidified frictional melts) have provided unequivocal evidence for past seismic slip on faults [Cowan, 1999]. Assuming a Newtonian rheology for frictional melts or conversion of mechanical work during earthquake faulting into heat, coseismic shear stress has been estimated from pseudotachylytes [Sibson, 1975; Di Toro *et al.*, 2005; Ujiie *et al.*, 2007; Kirkpatrick *et al.*, 2012]. However, pseudotachylytes are rarely preserved in their original state due to subsequent recrystallization, alteration, and deformation [Kirkpatrick and Rowe, 2013]. Vitrinite reflectance is an indicator of the thermal maturation of carbonaceous material. O'Hara [2004] identified the increased vitrinite reflectance from coal-bearing faults with the generation of frictional heat and estimated coseismic shear stress using the kinetic model of vitrinite reflectance and the thermal modeling. The increase of vitrinite reflectance on short timescales (comparable to 10 s earthquake rise time) was also confirmed by high-velocity friction experiments on carbonaceous materials [O'Hara *et al.*, 2006] or coal-bearing fault gouges [Kitamura *et al.*, 2012; Furuichi *et al.*, 2015]. In this study, we examine whether Raman spectra of carbonaceous material (RSCM) can be useful for the detection of past frictional heating on faults and the estimation of coseismic shear stress.

RSCM have been used to estimate the maximum attained temperatures in sedimentary and metamorphic rocks [e.g., Beyssac *et al.*, 2002; Aoya *et al.*, 2010; Kouketsu *et al.*, 2014]. Recent studies on high-velocity friction experiments have indicated that coal maturation and graphitization on carbonaceous-bearing fault gouges occurred when the power densities ($\Phi(t)=\tau(t)V(t)$, where V and t are slip rate and time, respectively) were ≥ 0.52 MW/m² and >10 MW/m², respectively [Ohashi *et al.*, 2011; Kuo *et al.*, 2013; Furuichi *et al.*, 2015]. These results suggest that RSCM are useful indicators of frictional heating on faults. However, it has not been tested whether RSCMs are utilized for detecting increased heating from natural faults. In this study, we

investigated RSCM utilization for the argillite-derived pseudotachylytes in the Shimanto accretionary complex in southwest Japan [Ujiie *et al.*, 2007]. We also examined RSCM in experimentally generated pseudotachylytes, resulting from the frictional melting of the argillite (host rock of the pseudotachylytes in the Shimanto accretionary complex) at seismic slip rates [Ujiie *et al.*, 2009]. Since these natural and experimental pseudotachylytes originate from the frictional melting of terrigenous argillaceous rocks, carbonaceous material is expected to be included in pseudotachylytes. Natural pseudotachylytes in accretionary complexes are commonly altered in fluid-saturated fault zones [Ujiie and Kimura, 2014]. Thus, the investigation of RSCM of experimental pseudotachylytes provides invaluable opportunities to assess the effect of alteration on RSCM and the correlation between the magnitude of shear stress and RSCM.

2. Raman Spectroscopic Analysis of Pseudotachylytes

2.1. Natural and Experimental Pseudotachylytes

The pseudotachylyte-bearing fault zone develops at the top of the Mugí mélangé in the Late Cretaceous Shimanto accretionary complex of eastern Shikoku, southwest Japan, which bounds offscraped coherent turbidites above from underplated tectonic mélangé below [Ujiie *et al.*, 2007] (supporting information S1). The fault zone is interpreted to form when the plate-boundary faulting is localized at the top of the subducting mélangé or shearing along the roof thrust of duplex structures at depths of 4–6 km. The pseudotachylyte-bearing dark veins are typically ~1 mm thick and sharply cut the foliated cataclasite derived from the argillaceous mélangé (supporting information S1). Under plane-polarized light, the pseudotachylytes are marked by the presence of subangular to subrounded grains of quartz and feldspar, and small dark grains (mainly carbonaceous materials) in the transparent matrix (Figures 1a and 1b). The pseudotachylyte matrix is dark and optically isotropic under cross-polarized light. Under a scanning electron microscope (SEM) and transmission electron microscope (TEM), embayed and rounded margins of albite and K-feldspar grains, vesicles, and idiomorphic acicular microlites of mullite or muscovite are observed in the glassy matrix of illite composition (Figure 1c), suggesting that frictional melting occurred at temperatures higher than 1100°C [Ujiie *et al.*, 2007; Ujiie and Kimura, 2014]. The pseudotachylyte matrix mostly suffered devitrification and alteration, but the pseudotachylyte-bearing dark veins locally preserve the embayed boundaries and contain the unaltered pseudotachylytes survived from alteration (Figures 1a and 1b).

The experimental pseudotachylytes were generated from high-velocity friction experiments on argillite [Ujiie *et al.*, 2009]. Experiments were conducted on a rotary shear, high-velocity friction apparatus at Kyoto University (the apparatus is now at Yamaguchi University) under room humidity conditions at room temperature and normal stresses (σ_n) of 2.7–13.3 MPa (supporting information S1). A pair of solid argillite cylinders with a diameter of 25 mm was set in the apparatus in which one cylinder was rotated parallel to the foliation in argillite by a servomotor while the other cylinder remained stationary. Specimens were jacketed with an aluminum ring to avoid sample destruction by thermal fracturing. Given the configuration of a rotary shear experiment with solid cylindrical specimens, the slip rate varied from zero at the center to the maximum at the edge. We used an equivalent slip rate (V_e), defined such that V_e multiplied by the sliding surface area (S) provides the rate of frictional work, assuming a constant shear stress over S [Shimamoto and Tsutsumi, 1994]. The calculated V_e for experiments was 1.1 m/s. The experimental conditions and results are shown in Table S1. Experiments showed slip weakening and subsequent slip strengthening (Figure 1d), which occurred in association with the formation of melt patches and the growth (thickening) of the melt layer, respectively [Ujiie *et al.*, 2009]. After each experiment, a pair of solid argillite cylinders was welded due to the solidification of the frictional melt (i.e., experimental pseudotachylyte). The sample assembly was cut through the axis of the cylinder to make a thin section that was perpendicular to the slip direction and pseudotachylyte (supporting information S1).

Experimental pseudotachylytes show the nearly the same features as unaltered natural pseudotachylytes; embayed and rounded margins of albite and K-feldspar grains and vesicles are present in the glassy matrix, suggesting frictional melting at temperatures $\geq 1100^\circ\text{C}$ [Ujiie *et al.*, 2009]. Under plane-polarized light, dark layers develop outside of pseudotachylyte (Figure 1e). Quartz veins in argillite are sharply cut by pseudotachylyte but preserved in dark layers, indicating that the dark layers outside pseudotachylyte were not involved in shear deformation. Under cross-polarized light, the dark layer matrix is optically isotropic and has the chemical composition of illite. Under SEM, the dark layers contain vesicles, but embayed and

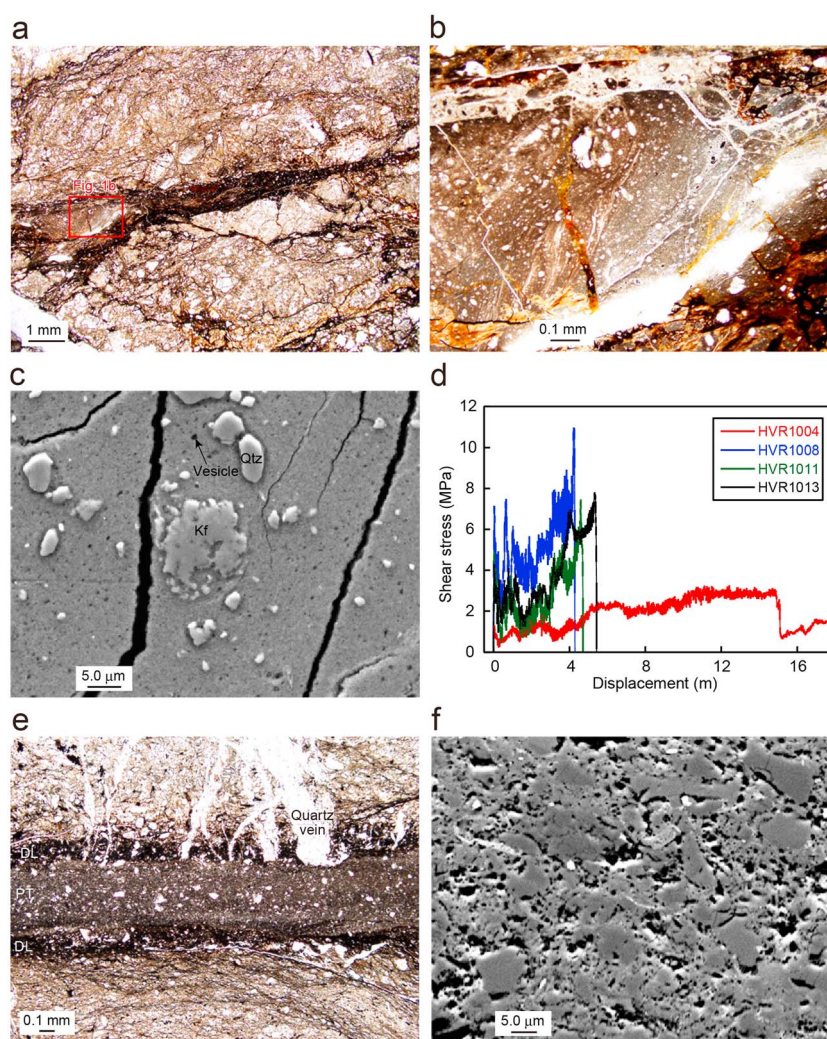


Figure 1. Natural and experimental pseudotachyrites. (a) The pseudotachylyte-bearing dark vein under plane-polarized light. (b) The pseudotachylyte surviving alteration, which is marked by the transparent matrix under plane-polarized light. Location of the photo is shown in Figure 1a. (c) Backscattered electron image of pseudotachylyte showing the embayed K-feldspar (Kf) grain and vesicles in the homogeneous, glassy matrix. While the K-feldspar grain shows marginal melting, the quartz (Qtz) grain preserves a sharp boundary, suggesting that the temperature during friction melting is higher than the melting temperature of K-feldspar (1150°C) but lower than that of quartz (1730°C). (d) Experimental results for argillite at 1.1 m/s plotted as shear stress versus displacement. (e) Experimental pseudotachylyte (PT) and dark layers (DL) developed along the margins of pseudotachylyte. (f) Backscattered electron image of the dark layer showing the irregularly shaped vesicles (dark portions) in the matrix.

rounded margins of grains are absent (Figure 1f). These features are recognized when illite is dehydrated and decomposed at ~850–1000°C [Grim and Bradley, 1940; McConville and Lee, 2005]. The dark layers likely represent the heat zones along the margins of the melt layer, which result from rapid heat conduction from the viscous shear zone [Ujii et al., 2009].

2.2. Raman Spectra

RSCM were obtained using a laser Raman microscope installed at the University of Tokyo equipping a 50X objective lens and a 514.5 nm Ar⁺ laser. Since the incident laser can increase the sample temperature and cause damage of carbonaceous material (CM), the laser power at the sample surface was set at approximately 0.7 mW, and the acquisition time was 30 s. We used thin sections made from natural and experimental pseudotachyrites for the Raman spectroscopic analysis. To prevent error due to the damage associated with the mechanical polishing during thin section preparation, only CM grains completely embedded within the host

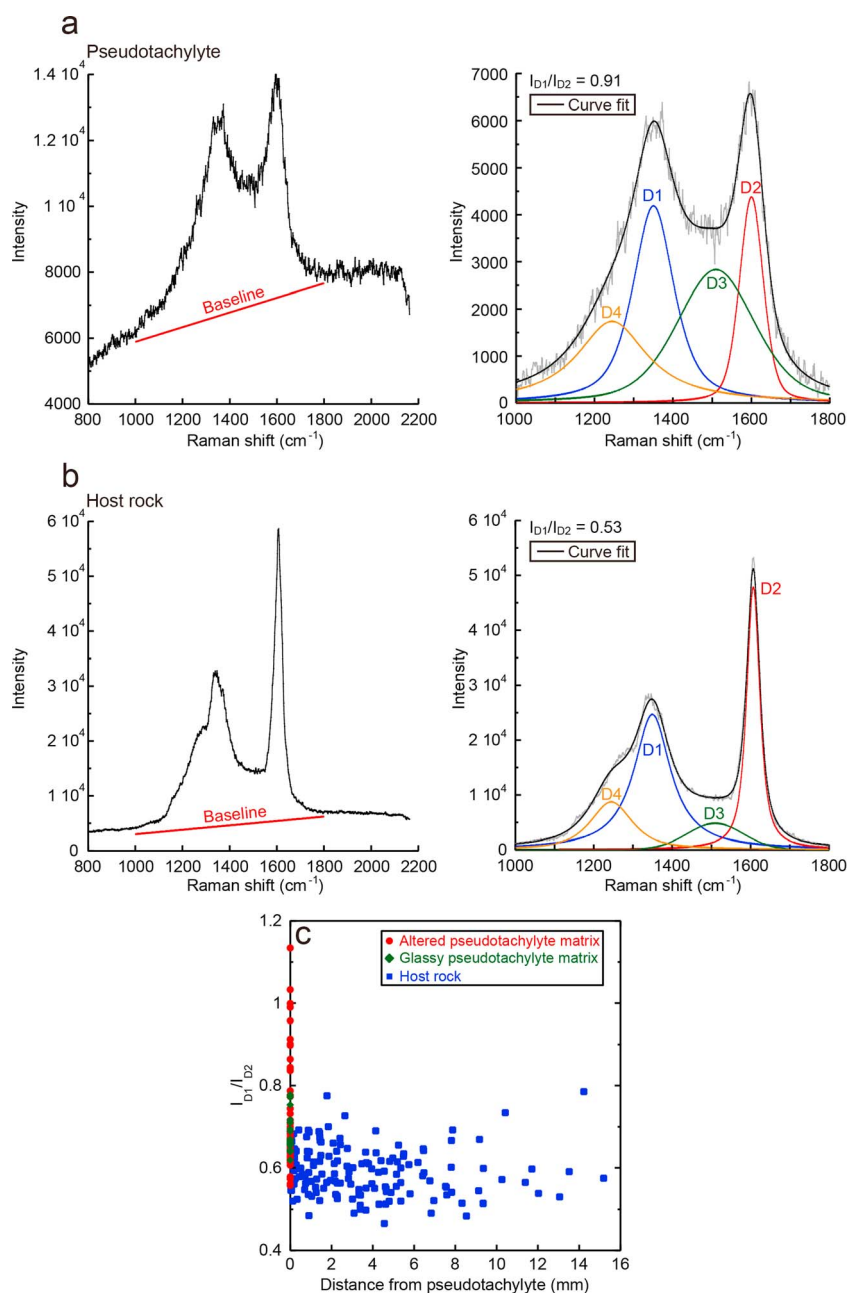


Figure 2. Representative Raman spectra and decomposed peaks of CM for (a) pseudotachylyte and (b) host rock. (c) Spatial distribution of I_{D1}/I_{D2} in pseudotachylyte and host rock plotted as a function of the distance from pseudotachylyte.

rocks or the matrices of pseudotachylyte and dark layers were used for the Raman measurements. Peak decomposition was carried out on the obtained Raman spectra using a commercial software PeakFit 4.12 (Systat Software, Inc.). Representative RSCM in natural pseudotachylyte and host rock are shown in Figures 2a and 2b, respectively. Since a fluorescent background was present, the linear baseline was subtracted in the range of 1000–1800 cm⁻¹. Then, the spectra were decomposed into D1-, D2- (or G-), D3-, and D4-bands for CM with a pseudo-Voigt function (Gaussian-Lorentzian Sum), which have peak positions near 1350 cm⁻¹, 1590 cm⁻¹, 1510 cm⁻¹, and 1245 cm⁻¹, respectively [e.g., Sadezky *et al.*, 2005; Lahfid *et al.*, 2010; Kouketsu *et al.*, 2014]. Peak positions, intensities, and half widths were optimized except for the peak positions of D3 and D4, which were fixed. The thermal maturation of CM was evaluated based on the intensity (i.e., height) ratio of curve fit at the frequencies corresponding to the positions of D1- and D2-bands.

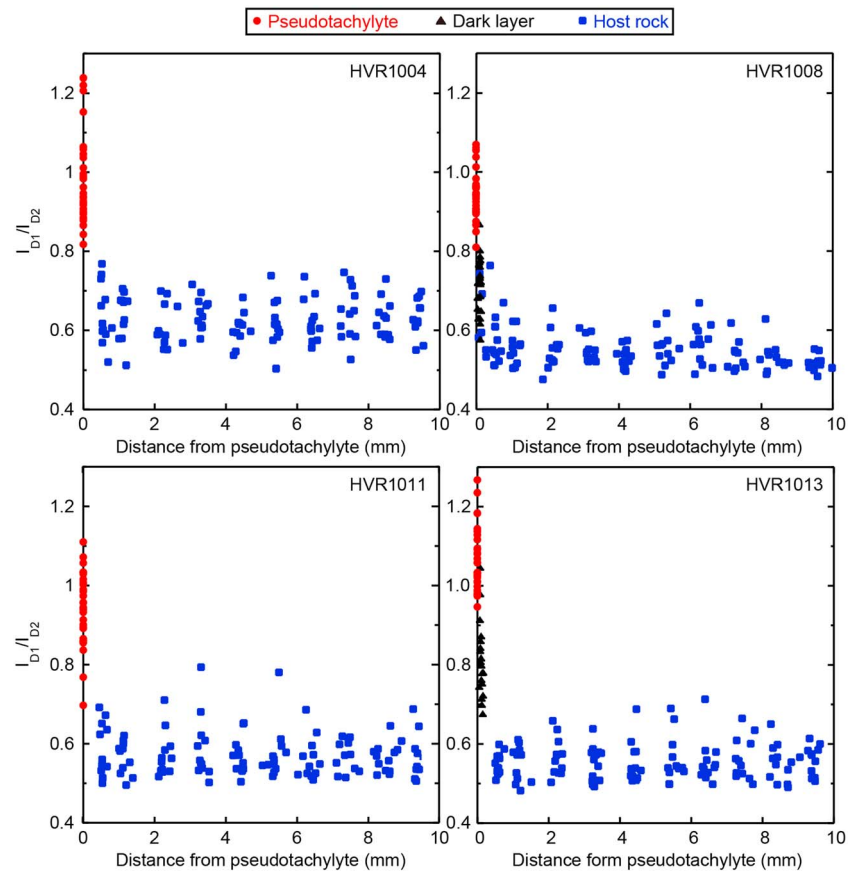


Figure 3. Spatial distribution of I_{D1}/I_{D2} in experimental pseudotachylytes, dark layers, and host rocks plotted as a function of the distance from pseudotachylyte. We cannot measure the RSCM in the dark layers for HVR1004 and HVR1011 because of the broken marginal portions of the specimen and the poorly developed dark layers, respectively.

3. Results

The RSCM in the host rock show prominent peaks attributable to the D1- and D2-bands, with the I_{D1}/I_{D2} values ranging from ~ 0.5 to 0.7 (Figures 2b and 2c). The average I_{D1}/I_{D2} value in the host rock is 0.59 with a standard deviation (SD) of 0.06 . The RSCM in the pseudotachylyte-bearing dark vein are characterized by an increase in height of the D1-band (Figure 2a). The I_{D1}/I_{D2} values in the pseudotachylyte-bearing dark vein vary but are higher (~ 0.7 – 1.1) than the host rock (Figure 2c). The average I_{D1}/I_{D2} value in the pseudotachylyte-bearing dark vein is as high as 0.71 (SD 0.12). Such increased height of the D1-band and increased I_{D1}/I_{D2} values are observed when carbonization is increased from low-grade CM (amorphous carbon) to medium-grade CM (transitional material between amorphous carbon and crystallized graphite) [Kouketsu *et al.*, 2014]. The range of I_{D1}/I_{D2} values in unaltered pseudotachylytes is similar to that in altered pseudotachylytes (Figure 2c).

As in natural pseudotachylytes, the RSCM in experimentally generated pseudotachylytes and the dark layers outside pseudotachylytes show increased carbonization, which is exhibited by an increase in the height of the D1-band and an increase in the I_{D1}/I_{D2} values with respect to the host rocks (Figure 3). The I_{D1}/I_{D2} values in pseudotachylytes do not show systematic radial change from the center to the edge of the solid cylindrical specimen or roughly increase with the radial distance (supporting information S1). Average I_{D1}/I_{D2} values in pseudotachylytes are 0.94 – 1.06 (SD 0.06 – 0.11). Dark layers exhibit lower I_{D1}/I_{D2} values than pseudotachylytes, with average I_{D1}/I_{D2} values of 0.71 – 0.81 (SD 0.07 – 0.09).

To investigate the relationship between frictional work (W), average shear stress (τ_{av}) and average I_{D1}/I_{D2} values, W is determined by calculating the integral of the shear stress (τ) versus displacement, from zero to the end of the experiment (total displacement, δ_f):

$$W = \int_0^{\delta_f} \tau(\delta) d\delta. \quad (1)$$

τ_{av} is obtained by dividing W by δ_f . The results indicate that there are no correlations between W , τ_{av} , and the average I_{D1}/I_{D2} values (Figures 4a and 4b). However, a clear negative correlation is observed between τ_{av} and the SD of average I_{D1}/I_{D2} values (I_{sd}) (Figure 4c). The best fit regression curve determined from the KaleidaGraph software is expressed by

$$I_{sd} = 0.17 \cdot \tau_{av}^{-0.57} \quad (R^2 = 1.0). \quad (2)$$

This relationship indicates that I_{sd} exponentially decreases with an increase in τ_{av} .

4. Discussion

The results of Raman spectroscopic analysis demonstrate that carbonization is more progressed in experimental pseudotachylytes and dark layers than in host rocks, which suggests increased heating along pseudotachylytes and dark layers. Although the heating rate is expected to increase from the center to the edge of the solid cylindrical specimen, the spatial distribution of I_{D1}/I_{D2} values in pseudotachylytes indicates that there is no clear radial increase in carbonization. This may reflect the mixing flow of frictional melt during experiments. The rough correlation between I_{D1}/I_{D2} values and radial distance (HVR 1011 in the supporting information) might be caused by the insufficient mixing flow. Compared to dark layers, carbonization is more advanced in pseudotachylytes. This is consistent with the formation of pseudotachylytes resulted from frictional melting at temperatures $\geq 1100^\circ\text{C}$, while dark layers represent the dehydration and decomposition of illite at $\sim 850\text{--}1000^\circ\text{C}$ [Ujii *et al.*, 2009]. The dark layers are not shear zones but rather result from heat conduction from the melt zone. The duration of experiments is $\sim 4\text{--}16$ s. These features indicate that RSCM can detect short-lived thermal events such as frictional heating on faults, at least when the temperatures are high enough to induce thermal decomposition of illite.

RSCM in pseudotachylytes and host rocks are similar to RSCM in samples RS9 (medium-grade CM) and Kr6 (low-grade CM) of Kouketsu *et al.* [2014], respectively, whose maximum temperatures determined from the RSCM geothermometer are $301 \pm 30^\circ\text{C}$ and $165 \pm 35^\circ\text{C}$, respectively. The maximum temperatures of host rocks are consistent with those determined from vitrinite reflectance [Ikesawa *et al.*, 2005]. However, the maximum temperatures of pseudotachylytes are much lower than temperatures during frictional melting ($\geq 1100^\circ\text{C}$) [Ujii *et al.*, 2007, 2009]. Thus, the RSCM geothermometer cannot be applied to the estimation of temperatures during frictional melting on faults. Recently, Pawlyta *et al.* [2015] heated CM up to 2600°C for 30 min under an argon flow and found that only a partial graphitization took place. The RSCM after heating at 1500°C is similar to those in pseudotachylytes, but Pawlyta *et al.* [2015] did not conduct heating experiments below 1500°C . Further heating experiments at lower temperatures are needed to evaluate maximum temperatures from RSCM in pseudotachylytes.

The RSCM geothermometer indicated that the increased I_{D1}/I_{D2} values are recognized for medium-grade CM, whose maximum temperatures range from 280°C to 400°C [Kouketsu *et al.*, 2014]. For high-grade CM at temperatures above 400°C , the prominent peak of G-band arises, and the intensities of D1- and D2-bands decrease with increasing temperature [e.g., Beyssac *et al.*, 2002; Kouketsu *et al.*, 2014]. Thus, when the ambient temperatures are higher than 280°C , the CM in host rocks are too thermally mature to detect the increased heating on faults. Detection of past frictional heating on faults using RSCM is, therefore, most practical in low-grade CM-bearing host rocks, in which I_{D1}/I_{D2} values remain small with ambient temperatures lower than 280°C .

The similar range of I_{D1}/I_{D2} values between unaltered and altered pseudotachylytes and the increased I_{D1}/I_{D2} values of > 0.7 in natural and experimental pseudotachylytes suggest that increased carbonization is preserved even after devitrification and alteration. This may reflect the fact that thermal maturation of CM is an irreversible reaction not only for heating in geological time scales but also for short-lived thermal events.

Under the high-velocity friction experiments at σ_n of $2.7\text{--}13.3$ MPa, average I_{D1}/I_{D2} values do not correlate with W and τ_{av} . Absence of correlation can also be expected between average I_{D1}/I_{D2} values and the power density ($\Phi(t)$), because $\Phi(t)$ is expressed as $\Phi(t) \approx \tau_{av} \cdot 1.1$. When diffusive heat loss is limited to adjacent rocks during a short-time coseismic slip, the rate of temperature rise (dT/dt) is proportional to $\Phi(t)$ (or τ_{av})

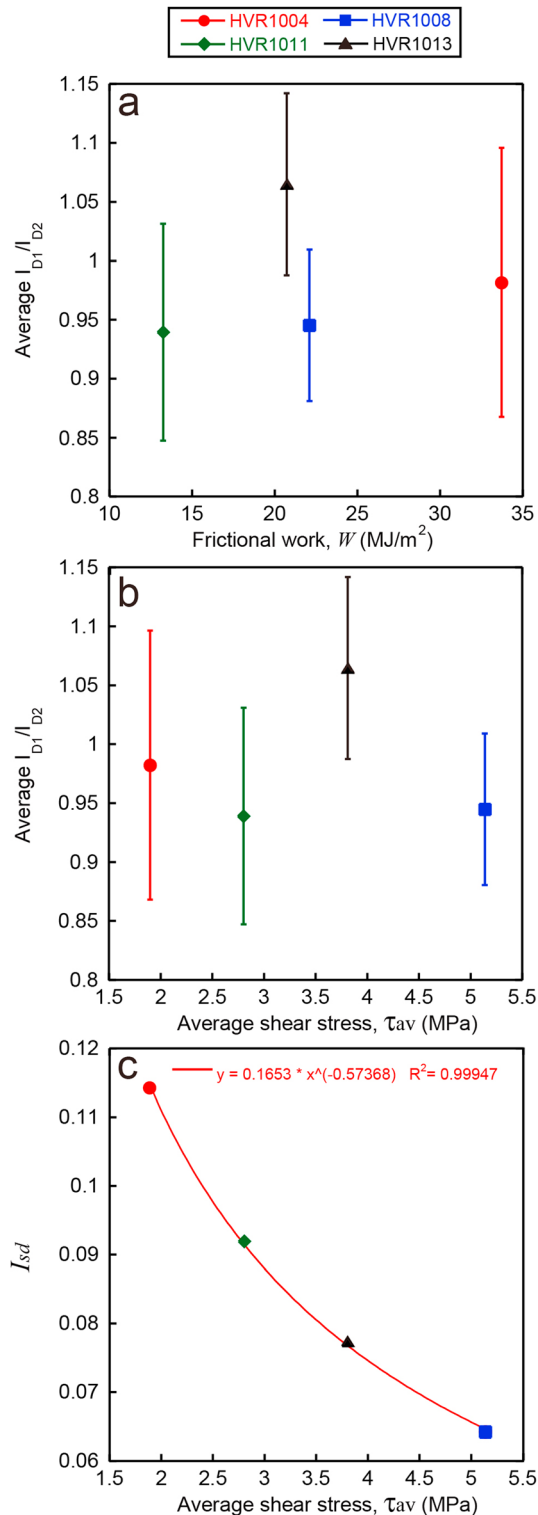


Figure 4. The comparison between high-velocity friction experiment data and Raman data. The error bars in Figures 4a and 4b indicate the standard deviation (SD) of average l_{D1}/l_{D2} values. (a) The relationship between frictional work (W) and average l_{D1}/l_{D2} values in pseudotachylytes. (b) The relationship between average shear stress (τ_{av}) and average l_{D1}/l_{D2} values in pseudotachylytes. (c) The relationship between τ_{av} and SD of average l_{D1}/l_{D2} values (l_{sd}) in pseudotachylytes.

[Rice, 2006; Di Toro *et al.*, 2011]. The range of $\tau_{av} = 1.9$ –5.1 MPa in Figure 4b may be too small to result in a dependence of average l_{D1}/l_{D2} values on τ_{av} or dT/dt . The negative correlation between l_{sd} and τ_{av} suggests that increased dT/dt due to high $\Phi(t)$ (or τ_{av}) reduced the heterogeneity of the thermal maturation of CM in the melt zone, resulting in a decrease in l_{sd} . Natural pseudotachylyte exhibits lower average l_{D1}/l_{D2} value and higher l_{sd} than experimental pseudotachylytes, which could reflect the lower τ_{av} value in natural pseudotachylyte than in experimental one. The previous chemical analysis of natural and experimental pseudotachylytes suggests that natural pseudotachylytes show nearly the same the chemical composition as experimental ones but are more hydrous [Ujiie *et al.*, 2009]. The higher water content leads to a lower viscosity of frictional melt, thereby reducing τ_{av} in natural pseudotachylytes. The higher l_{sd} in natural pseudotachylytes may also reflect shorter earthquake slip durations compared to the duration of the high-velocity friction experiments (~ 4 –16 s), which could result in a lower probability to homogenize the thermal maturation of CM in the melt zone.

The coseismic shear stress of natural pseudotachylytes estimated from equation (2) is 1.8 MPa. Assuming the hydrostatic pressure in the horizontal pseudotachylyte-bearing fault zone at depths of 4–6 km, the effective normal stress for a rock density (ρ) of 2500 kg/m³ is ~ 38 –57 MPa. The resulting apparent friction coefficient is ~ 0.03 –0.05. This suggests the melt lubrication during the earthquakes at depths of 4–6 km in the subduction zone. Assuming most of the mechanical work during earthquake faulting is converted into heat, τ_{av} can be expressed as

$$\tau_{av} = p[C_p(T_m - T_{hr}) + (1 - \phi)H]w/d \quad (3)$$

where C_p is the specific heat at constant pressure, T_m is the melting temperature, T_{hr} is the host rock temperature, ϕ is the volume fraction of unmelted grains, H is the latent heat of fusion, w is the thickness of slipping zone, and d is the coseismic

fault displacement. Given $C_p = 1000 \text{ J/kg } ^\circ\text{C}$, $T_m = 1100^\circ\text{C}$, $T_{hr} = 180^\circ\text{C}$, $\phi = 0.09\text{--}0.26$, $H = 3.2 \cdot 10^5 \text{ J/kg}$, and $w = 1 \text{ mm}$ [Ujiie et al., 2007], d is $\sim 1.6\text{--}1.7 \text{ m}$. This suggests the existence of $\sim M7$ earthquakes [Sibson, 1989] in the subduction zone.

5. Conclusions

On the basis of increased carbonization in natural and experimental pseudotachylytes derived from argillite in the Shimanto accretionary complex, we suggest that RSCM is useful for detecting increased heating on faults that have temperatures at least high enough to induce thermal decomposition of illite at $\sim 850\text{--}1000^\circ\text{C}$. The increased carbonization is preserved even after devitrification and alteration of the pseudotachylyte matrix. This may reflect that thermal maturation of CM during short-lived thermal events such as friction heating is an irreversible reaction.

The comparison between high-velocity friction experiment data and Raman data indicates that there are no correlations between W , τ_{av} , and average I_{D1}/I_{D2} values. A negative correlation between τ_{av} and I_{sd} in pseudotachylytes suggests that when dT/dt is increased due to high τ_{av} , thermal maturation degree of CM in the melt zone tends to be more uniform. The coseismic shear stress estimated from the negative correlation is 1.8 MPa , which yields that an apparent friction coefficient under hydrostatic conditions at depths of $4\text{--}6 \text{ km}$ is $\sim 0.03\text{--}0.05$. When the ambient temperature is lower than 280°C , RSCM in pseudotachylytes will be useful for estimation of coseismic fault strength.

Acknowledgments

The Raman data and high-velocity friction experiment data are available from the first and second authors upon request. We thank GRL Editor Andrew V. Newman, Ake Fagereng, and two anonymous reviewers for helpful suggestions and comments. We also thank Mao Watanabe and Hiroki Tabata for their assistance with Raman spectroscopic analysis. K.U. is supported by the Grant-in-Aid for Scientific Research (B) from JSPS (26287124) and JSPS KAKENHI grant JP16H06476.

References

- Aoya, M., Y. Kouketsu, S. Endo, H. Shimizu, T. Mizukami, D. Nakamura, and S. Wallis (2010), Extending the applicability of the Raman carbonaceous-material geothermometer using data from contact metamorphic rocks, *J. Metamorph. Geol.*, **28**, 895–914.
- Beyssac, O., B. Goffé, C. Chopin, and J. N. Rouzaud (2002), Raman spectra of carbonaceous material in metasediments: A new geothermometer, *J. Metamorph. Geol.*, **20**, 859–871.
- Cowan, D. S. (1999), Do faults preserve a record of seismic slip? A field geologist's opinion, *J. Struct. Geol.*, **21**, 995–1001.
- Di Toro, G., G. Pennacchioni, and G. Teza (2005), Can pseudotachylytes be used to infer earthquake source parameters? An example of limitations in the study of exhumed faults, *Tectonophysics*, **402**, 3–20.
- Di Toro, G., R. Han, T. Hirose, N. De Paola, S. Nielsen, K. Mizoguchi, F. Ferri, M. Cocco, and T. Shimamoto (2011), Fault lubrication during earthquakes, *Nature*, **471**, 494–498, doi:10.1038/nature09838.
- Fulton, P. M., et al. (2013), Low coseismic friction on the Tohoku-Oki fault determined from temperature measurements, *Science*, **342**, 1214–1217, doi:10.1126/Science.1243641.
- Furuichi, H., K. Ujiie, Y. Kouketsu, T. Saito, A. Tsutsumi, and S. Wallis (2015), Vitrinite reflectance and Raman spectra of carbonaceous material as indicators of frictional heating on faults: Constraints from friction experiments, *Earth Planet. Sci. Lett.*, **424**, 191–200, doi:10.1016/j.epsl.2015.05.037.
- Grim, R. E., and W. F. Bradley (1940), Investigation of the effect of heat on the clay minerals illite and montmorillonite, *J. Am. Ceram. Soc.*, **23**, 242–248.
- Ikesawa, E., G. Kimura, K. Sato, K. Ikehara-Ohmori, Y. Kitamura, A. Yamaguchi, K. Ujiie, and Y. Hashimoto (2005), Tectonic incorporation of the upper part of oceanic crust to overriding plate of a convergent margin: An example from the Cretaceous-early Tertiary Mugli Mélange, the Shimanto Belt, Japan, *Tectonophysics*, **401**, 217–230.
- Kirkpatrick, J. D., and C. D. Rowe (2013), Disappearing ink: How pseudotachylytes are lost from the rock record, *J. Struct. Geol.*, **52**, 183–198.
- Kirkpatrick, J. D., K. J. Dobson, D. F. Mark, Z. K. Shipton, E. E. Brodsky, and F. M. Stuart (2012), The depth of pseudotachylyte formation from detailed thermochronology and constraints on coseismic stress drop variability, *J. Geophys. Res.*, **117**, B06406, doi:10.1029/2011JB008846.
- Kitamura, M., H. Mukoyoshi, P. M. Fulton, and T. Hirose (2012), Coal maturation by frictional heat during rapid fault slip, *Geophys. Res. Lett.*, **39**, L16302, doi:10.1029/2012GL052316.
- Kouketsu, Y., T. Mizukami, H. Mori, S. Endo, M. Aoya, H. Hara, D. Nakamura, and S. Wallis (2014), A new approach to develop the Raman carbonaceous material geothermometer for low-grade metamorphism using peak width, *Isl. Arc*, **23**, 33–50.
- Kuo, L.-W., H. Li, S. A. F. Smith, G. Di Toro, J. Suppe, S.-R. Song, S. Nielsen, H.-S. Sheu, and J. Si (2013), Gouge graphitization and dynamic fault weakening during the 2008 $M_w 7.9$ Wenchuan earthquake, *Geology*, **42**, 47–50.
- Lahfid, A., O. Beyssac, E. Deville, F. Negro, C. Chopin, and B. Goffé (2010), Evolution of the Raman spectrum of carbonaceous material in low-grade metasediments of the Glarus Alps (Switzerland), *Terra Nova*, **22**, 354–360.
- McConville, C. J., and W. E. Lee (2005), Microstructural development on firing illite and smectite clays compared with that in kaolinite, *J. Am. Ceram. Soc.*, **88**, 2267–2276.
- O'Hara, K. (2004), Paleo-stress estimates on ancient seismogenic faults based on frictional heating on coal, *Geophys. Res. Lett.*, **31**, L03601, doi:10.1029/2003GL018890.
- O'Hara, K., K. Mizoguchi, T. Shimamoto, and J. C. Hower (2006), Experimental frictional heating of coal gouge at seismic slip rates: Evidence for devolatilization and thermal pressurization of gouge fluids, *Tectonophysics*, **424**, 109–118.
- Ohashi, K., T. Hirose, and T. Shimamoto (2011), Shear-induced graphitization of carbonaceous materials during seismic fault motion: Experiments and possible implications for fault mechanics, *J. Struct. Geol.*, **33**, 1122–1134, doi:10.1016/j.jsg.2006.10.012.
- Pawlyta, M., J.-N. Rouzaud, and S. Duber (2015), Raman microspectroscopy characterization of carbon blacks: Spectral analysis and structural information, *Carbon*, **84**, 479–490.
- Rice, J. R. (2006), Heating and weakening of faults during earthquake slip, *J. Geophys. Res.*, **111**, B05311, doi:10.1029/2005JB004006.
- Sadezky, A., H. Muckenhuber, H. Grothe, R. Niessner, and U. Poschl (2005), Raman microspectroscopy of soot and related carbonaceous materials: Spectral analysis and structural information, *Carbon*, **43**, 1731–1742.

- Shimamoto, T., and A. Tsutsumi (1994), A new rotary-shear high-velocity frictional testing machine: Its basic design and scope of research (in Japanese with English abstract), *Struct. Geol.*, 39, 65–78.
- Sibson, R. H. (1975), Generation of pseudotachylite by ancient seismic faulting, *Geophys. J. R. Astron. Soc.*, 43, 775–794.
- Sibson, R. H. (1989), Earthquake faulting as a structural process, *J. Struct. Geol.*, 11, 1–14.
- Ujiie, K., and G. Kimura (2014), Earthquake faulting in subduction zones: Insights from fault rocks in accretionary prisms, *Prog Earth Planet Sci*, 1, 1–30, doi:10.1186/2197-4284-1-7.
- Ujiie, K., H. Yamaguchi, A. Sakaguchi, and S. Toh (2007), Pseudotachylites in an ancient accretionary complex and implications for melt lubrication during subduction zone earthquakes, *J. Struct. Geol.*, 29, 599–613.
- Ujiie, K., A. Tsutsumi, Y. Fialko, and H. Yamaguchi (2009), Experimental investigation of frictional melting of argillite at high slip rates: Implications for seismic slip in subduction-accretion complexes, *J. Geophys. Res.*, 114, B04308, doi:10.1029/2008JB006165.
- Ujiie, K., et al. (2013), Low coseismic shear stress on the Tohoku-Oki megathrust determined from laboratory experiments, *Science*, 342, 1211–1214, doi:10.1126/science.1243485.